Available online www.jsaer.com

***Journal of Scientific and Engineering Research*, 2023, 10(8):82-89**

Research Article

ISSN: 2394-2630
CODEN(USA): JSERBR

Numerical Study to determine the Effect of Open Window on Aerodynamic Drag, Lift, Fuel Consumption and CO_2 Emission of Minibus

Olusola Oloruntoba[*1], Akintayo Akinkunmi[1]

[1]Department of Automotive Engineering, Elizade University, P.M.B. 002, Ilara-Mokin, Ondo State, Nigeria
Email: olusola.oloruntoba@elizadeuniversity.edu.ng

Abstract Aerodynamic drag of vehicle affects fuel consumption, CO_2 emission as well as stability and safety. Modification of geometry has been shown to have significant impact on aerodynamic drag. Since window opening is common for commercial minibus in tropical Africa, such as Nigeria, there is need to investigate the effect of window opening on the vehicle. The main objective of this project is to investigate the effect of window opening on aerodynamic drag, lift, fuel consumption and CO_2 emission of typical minibus. The impact of window opening on the drag characteristics of a three-dimensional commercial buses model was numerically investigated using ANSYS Fluent CFD software at vehicle speed between 40 km/h and 140 km/h, at 20 km/h interval. The findings show that aerodynamic drag and lift remain relatively constant with variation with speed. However, aerodynamic drag and lift of open window minibus are, 10.10 % and 48.65 % respectively, higher than values for the closed window minibus. This is reflected in 10.56 % increase fuel consumption and CO2 emission. Also, the increase in lift would affect tire grip, stability and safety.

Keywords Aerodynamic drag, Lift, Open Window, Fuel Consumption, CO_2 Emission.

1. Introduction

Vehicle aerodynamics studies the movement of air in and around a vehicle that affects its stability and safety. The balance of forces such as thrust, weight, lift and drag are generated. Drag or aerodynamic drag resists the movement of the vehicle and lift elevates the vehicle off the ground. The purpose of aerodynamic research is to minimize air resistance or aerodynamic drag. Previous CFD simulations showed that driving at low speed with windows open uses less fuel than using air conditioning [1]. However, opening windows and increasing speed increases air resistance, power consumption, CO_2 emissions, and interior noise.

Vehicle aerodynamics play an important role in fuel efficiency. In another study, wind tunnel experimentation and CFD were used to examine the effect of *open window* on drag conditioning [1]. The results showed that vehicles with the *open window* have higher values of drag coefficient. However, that was no direct relation between window opening and drag coefficient. The report of an experimental and CFD study showed a consistent air flow pattern for bus with *open window* [2].

Increasing global demand for energy has led to soaring fuel prices, and it is also necessary to reduce fuel consumption of road vehicles in order to deal with environmental pollution problems. One obvious approach to achieve this is to reduce aerodynamic drag, which consequently improves fuel efficiency. In Nigeria, commercial minibus and bus operators mostly leave their windows open. This has the potential to vary vehicle geometry and consequently affect aerodynamic drag, lift, fuel consumption, CO_2 emissions, stability and safety [3], [4]. A previous work similar to the present study was carried out for large bus, and their findings showed increase in aerodynamic drag and lift when windows are open [5].

This study aims to investigate the effects of *open window* on aerodynamic drag, lift, fuel consumption and CO_2 emissions of a typical commercial minibus in Nigeria. In order to achieve this, a CFD simulation study is performed. The 2020 model of Toyota HiAce minibus is analysed using computational fluid dynamics (CFD) techniques; an established fluid dynamics numerical approximation tool. ANSYS™ FLUENT™, a widely used and robust software, is used in this study.

2. Description of The Model

2.1 Problem Description

The investigation utilized a 2020 TOYOTA™ HiAce™ minibus, illustrated in Figure 1, which has a length of 5.915 m, a width of 1.950 m, and a height of 1.990 m. ANSYS™ DesignModeler™ was used to design a Computer Aided Drawing (CAD) model of the minibus. In order to simplify the vehicle geometry for CFD simulations, complex features were excluded, as they could complicate meshing and numerical simulation, as noted by [6], [7]. Figures 2 and 3 present a typical TOYOTA™ HiAce™ with both an open and *closed window*.

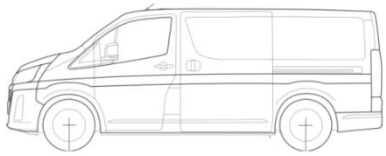

Figure 1: A graphical illustration of the 2020 model of TOYOTA™ HiAce™ minibus; (Source: [8]).

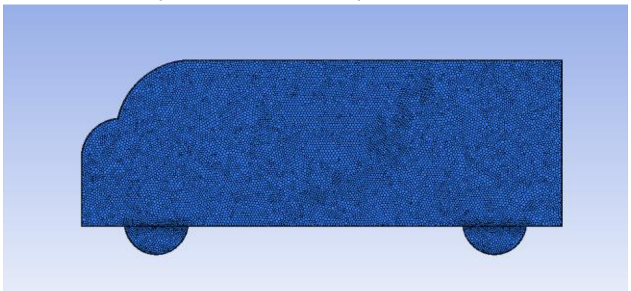

Figure 2: A simplified illustration of TOYOTA™ HiAce™ for closed window

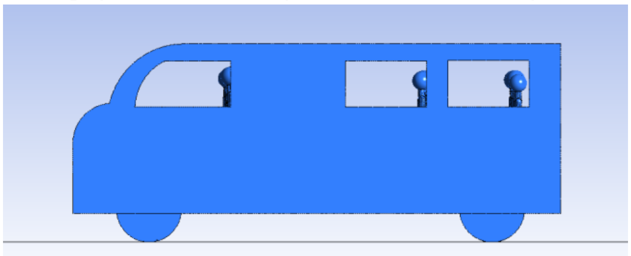

Figure 3: A simplified illustration of TOYOTA™ HiAce™ for open window

2.2 Numerical window tunnel test configuration

In order to simulate a realistic flow of air around the TOYOTA™ HiAce™ minibus, a numerical wind tunnel of considerable size is used, as described in previous studies [3], [7], [9]. Figure 4 shows Simplified TOYOTA™ HiAce™ minibus in a Numerical wind tunnel.

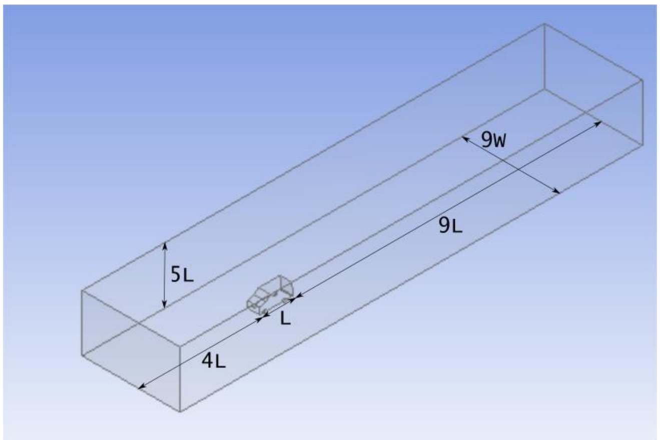

Figure 4: Simplified TOYOTA™ HiAce™ minibus in a Numerical wind tunnel; dimensions are shown in terms of vehicle length (L) and width (W); (Source: [3]).

2.3 Governing Equations

The Navier-Stokes equations (NSE) describe the aerodynamic flow of air around a vehicle. These equations include the conservation of mass and momentum, which are represented by Equations (1) and (2) respectively [7], [10].

$$\frac{\partial \rho}{\partial t} + \nabla \cdot (\rho \vec{v}) = 0 \tag{1}$$

where, $\vec{v}$, = velocity vector, ρ = density of air, P = static pressure, $\bar{\bar{\tau}}$ = stress tensor, and $\rho \vec{g}$ = gravitational body force. Turbulence is modelled using the SST $k - \omega$ viscous model [7], [10].

$$\frac{\partial (\rho \vec{v})}{\partial t} + \nabla \cdot (\rho \vec{v} \vec{v}) = -\nabla P + \nabla \cdot (\bar{\bar{\tau}}) + \rho \vec{g} \tag{2}$$

2.4 Boundary Conditions

The numerical wind tunnel is made up of conditions for velocity inlet and pressure outlet. The ground is simulated as a moving wall boundary that moves at the same speed as the velocity inlet. The top and side walls of the wind tunnel are considered as symmetry planes. There is a total of twelve cases, six of which have *open window* and the other six have *closed window*. These cases involve changing the inlet velocity in increments of 20km/h, ranging from 40km/h to 140km/h. The window opening and closing is also a factor in the cases.

2.5 Meshing

In this study, a polyhedral mesh was used for CFD simulations because this kind of mesh has cells that are connected to multiple neighbouring cells (as shown in Figure 5), resulting in better and more reliable approximations of gradients, faster convergence, and shorter computational time compared to tetrahedral and hexahedral mesh types [11]. Minimum mesh quality for the 12 cases studied is 0.217511.

Figure 5: Polyhedral mesh for vehicle speed $\boldsymbol{v} = 40\,\boldsymbol{km/h}$ and closed window.

2.6 Simulation

The governing equations are discretized numerically using the finite volume (FV) method. The Density-Based solver in ANSYS™ FLUENT™ is used for compressible flow. The flow is assumed to be in a steady-state, and the absolute velocity formulation is utilized. The SST $k - \omega$ viscous model is applied for turbulence. Implicit solution method is applied for pressure-velocity coupling. Spatial discretization of the gradient and flow is via the Least Square Cell Based and Second Order Upwind methods, respectively. Specific Dissipation Rate uses the First Order Upwind method.

2.7 Coefficients of Drag and Lift

Coefficients of drag and lift are described as shown in Equations (3) and (4) respectively, where the effects of inertia and road gradient are negligible [12].

$$C_d = \frac{2F_d}{\rho A_F v^2} \quad \textbf{(3)}$$

$$C_L = \frac{2F_L}{\rho A_L v^2} \quad \textbf{(4)}$$

2.8 Fuel Consumption

Equation (5) provides an approximation for the fuel efficiency of a vehicle that is traveling at a constant speed. Table (1) presents the assumed values for the symbols used in the equation.

$$q = \frac{F_d}{\eta_e \eta_t \rho_f H^*} \quad \textbf{(5)}$$

Table 1: Input values utilised to obtain fuel consumption for 12 cases of the minibus studied (Source: [3]).

S/N	Symbol	Value	Unit
1	η_e	0.32	dimensionless
2	η_t	0.94	dimensionless
3	ρ_f	740	kg/m^3
4	H^*	46.7	MJ/kg

2.9 CO_2 Emission

Equation (6) shows the direct relationship between fuel consumption and carbon dioxide emissions from vehicles, as stated by the *Environmental Protection Agency (EPA)* [13]. The *EPA's Green Vehicle Guide* provides an estimate of 8,887 grams of CO_2 emitted per gallon of gasoline, which is equivalent to $2.347 \times 10^6\ g$ per cubic meter.

$$E_{CO2} = (2.347 \times 10^6)q \quad \textbf{(6)}$$

3. Results and Discussion

3.1 Drag Coefficient

Total drag coefficient C_p of the minibus as it varies with vehicle speed between 40 km/h and 140 km/h, at 20km/h interval, is presented for both open and *closed window* conditions as shown in Figure 5. The figure shows that the *drag coefficient* C_p remains relatively constant for both scenarios regardless of vehicle speed. The corresponding average values of total drag coefficient are 0.6503 and 0.5907 for open and *closed window* scenarios respectively. This observed 10.10% increase in the value of C_p of the minibus for *open window*, over the corresponding value for *closed window* condition, is largely due to air flow in and around the vehicle cabin which led to increased pressure drag, the major contributor to the total drag coefficient of the minibus. Similar observations were recorded in previous studies [14], [15].

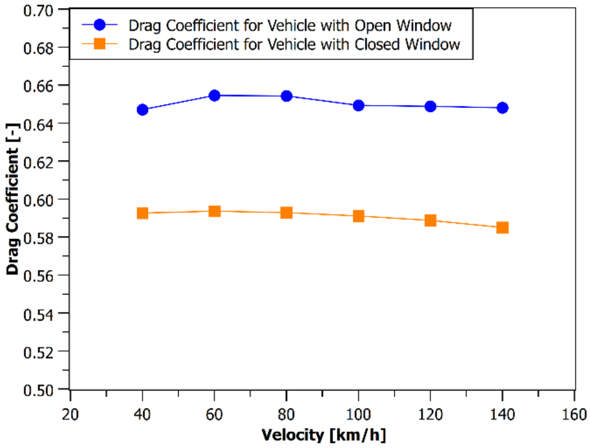

Figure 5: Total drag coefficient of minibus as a function of vehicle speed; open and closed window conditions.

3.2 Lift Coefficient

Figure 6 presents the plot of *lift coefficient* C_L of the minibus at various vehicle speed ranging between 40 km/h and 140 km/h, at 20km/h interval, for both open and *closed window* conditions. Similar to the observations for *drag coefficient*, *lift coefficient* C_L remains relatively constant for both window scenarios at different vehicle speed. The corresponding average values of *lift coefficient* are -0.0599 and -0.1167 for open and *closed window* scenarios respectively. This observed 48.65 % increase in the value of C_L of the minibus for *open window*, over the corresponding value for *closed window* condition, is largely due to air flow in and around the vehicle cabin which led to increased pressure in the vehicle cabin and hence lift of the minibus. As reported in previous studies, increase in drag results in corresponding increase in lift [5], [16]

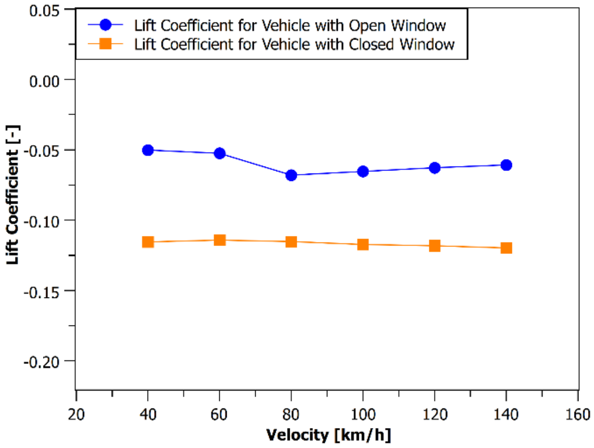

Figure 6: Lift coefficient of minibus as a function of vehicle speed; open and closed window conditions.

3.3 Fuel Consumption and CO2 Emission

Figure 7 shows the variation of fuel consumption of the minibus as a function of vehicle speed which varies between 40 km/h and 140 km/h, at 20km/h interval, for both open and *closed window* conditions. The quadratic increase in fuel consumption with respect to vehicle speed is due to the quadratic nature of the governing equation (Equation 3). However, the percentage increase in fuel consumption for *open window*, over the value for *closed window*, is observed to be approximately constant at 10.56 %; although increase in fuel consumption is quadratic as indicated in Figure 7.

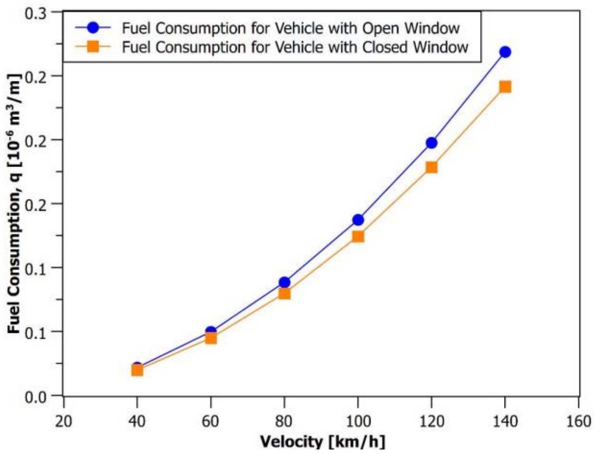

Figure 7: Fuel consumption of minibus at various vehicle Speeds/velocities at open and closed windows

Since CO_2 emission depends on fuel consumption, similar observations are noted in Figure 8, where percentage increase in CO_2 emission for *open window*, over the value for *closed window*, is also observed to be approximately constant at 10.56 %. Generally, fuel consumption and CO_2 emission of an *open window* is consistently higher than that of *closed window* irrespective to the speed, which means that more fuel is consumed and more CO_2 emitted when the windows are open during motion.

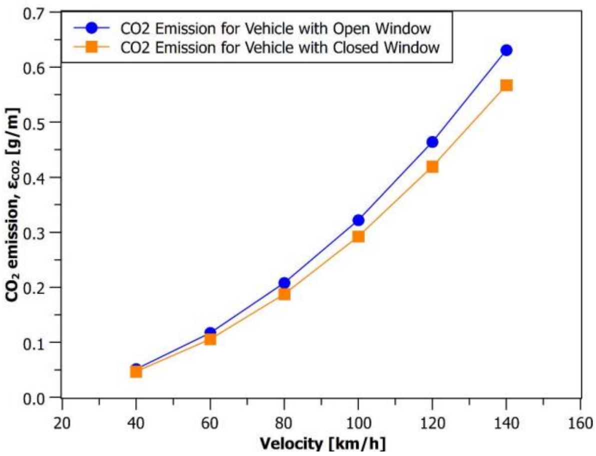

Figure 8: CO_2 emission of minibus at various vehicle speeds/velocities for open and closed windows

4. Conclusions

The impact of speed variations and the act of opening and closing windows on the aerodynamics, fuel usage, and CO_2 emissions of a minibus was examined using the ANSYS™ FLUENT™ software. The study involved a speed range of 40 km/h to 140 km/h, with intervals of 20 km/h. The investigation yielded the following observations:

- *Total drag coefficient* remains relatively constant, irrespective of speed, for both opened and *closed window* conditions. The corresponding average values of total drag coefficient are 0.6503 and 0.5907 for open and *closed window* scenarios respectively. Thus, *total drag coefficient* of minibus with *open window* consistently exceeded that of the *closed window* due to increased pressure in the cabin area owing to air flow.
- Similar to the observations for *drag coefficient*, *lift coefficient* C_L remains relatively constant for both window scenarios at different vehicle speed. The corresponding average values of *lift coefficient* are -0.0599 and -0.1167 for open and *closed window* scenarios respectively.

- Percentage increase in fuel consumption for *open window*, over the value for *closed window*, is observed to be approximately constant at 10.56 %; although increase in fuel consumption is quadratic. Similar observations are obtained for CO_2 emission.

Nomenclature

ν	=	Vehicle or minibus speed, [km/h]
$\vec{\nu}$	=	Velocity vector (of ν) [km/h]
g	=	Acceleration due to gravity, [m/s^2]
ρ	=	Density (of air) [kg/m^3]
P	=	Static pressure [N/m^3]
$\bar{\bar{\tau}}$	=	stress tensor [N/m^3]
$\rho\vec{g}$	=	Gravitational body force [kg/(ms)^2]
C_d	=	Total drag coefficient [-]
C_L	=	Lift coefficient [-]
q	=	Fuel consumption [10^{-6}m^3/m]
ε_{CO_2}	=	CO_2 emission [g/m]
η_e	=	Engine efficiency [-]
η_t	=	Transmission efficiency [-]
ρ_f	=	Density of fuel [kg/m^3]
F_d	=	Vehicle propulsion force [N]
F_L	=	Vehicle lift force [N]
A_F	=	Vehicle frontal area [m^2]
A_L	=	Vehicle lift area [m^2]
L	=	Length of minibus [m]
W	=	Width of minibus [m]
H	=	Height of minibus [m]
H^*	=	Thermal value of fuel [MJ/kg]

Acronyms

CO_2	=	Carbon dioxide
CFD	=	Computational Fluid Dynamics
NSE	=	Navier-Stokes Equations
FV	=	Finite Volume
EPA	=	Environmental Protection Agency

References

[1]. Y.-C. Zhang, J. Zhao, J. Li, and Z. Zhang, “Wind tunnel tests and aerodynamic numerical simulations of car opening windows,” Int. J. Veh. Des., vol. 58, no. 1, pp. 62–78, Jan. 2012, doi: 10.1504/IJVD.2012.045923.

[2]. S. R. Kale, S. V. Veeravalli, H. D. Punekar, and M. M. Yelmule, “Air flow through a non-airconditioned bus with open windows,” Sadhana, vol. 32, no. 4, pp. 347–363, Aug. 2007, doi: 10.1007/s12046-007-0029-3.

[3]. O. A. Oloruntoba and A. P. Okediji, “Effect of Speed and Boot Opening on Aerodynamics, Fuel Consumption, and CO2 Emission of Minibus,” FUOYE J. Eng. Technol., vol. 6, no. 4, Art. no. 4, Dec. 2021, doi: 10.46792/fuoyejet.v6i4.665.

[4]. O. Stopka, B. Šarkan, J. Vrabel, and J. Caban, “Investigation of fuel consumption of a passenger car depending on aerodynamic resistance and related aspects: a case study,” Arch. Motoryz., vol. 81, no. 3, pp. 129–136, Sep. 2018, doi: 10.14669/AM.VOL81.ART9.

[5]. K. Nikam and S. Borse, “Study of Air Flow through a Open Windows Bus Using OpenFOAM,” pp. 53–64, Jan. 2014.

[6]. A. Huminic and G. Huminic, "Aerodynamic Study of a Generic Car Model with Wheels and Underbody Diffuser," Int. J. Automot. Technol., vol. 18, no. 3, pp. 397–404, 2017, doi: 10.1007/s12239.

[7]. C. Zhang, C. P. Bounds, L. Foster, and M. Uddin, "Turbulence Modeling Effects on the CFD Predictions of Flow over a Detailed Full-Scale Sedan Vehicle," Fluids, vol. 4, no. 148, pp. 1–28, 2019, doi: 10.3390/fluids4030148.

[8]. Toyota, "Toyota HiAce Specification Data," Australia, 2020.

[9]. N. Ashton and A. Revell, "Comparison of RANS and DES Methods for the DrivAer Automotive Body Comparison of RANS and DES Methods for the DrivAer Automotive Body," SAE Int., 2015, doi: 10.4271/2015-01-1538.

[10]. ANSYS, ANSYS FLUENT Theory Guide, 17.0. Canonsburg, PA: ANSYS, Inc., 2016.

[11]. M. Sosnowski, J. Krzywanski, K. Grabowska, and R. Gnatowska, "Polyhedral meshing in numerical analysis of conjugate heat transfer," EPJ Web Conf., vol. 180, p. 02096, 2018, doi: 10.1051/epjconf/201818002096.

[12]. X. Zhang and C. Mi, Vehicle Power Management: Modelling, Control and Optimization. Springer, 2011. doi: 10.1007/978-0-85729-736-5.

[13]. Environmental Protection Agency, "Greenhouse Gas Emissions from a Typical Passenger Vehicle," Green Vehicle Guide, 2018. https://www.epa.gov/greenvehicles/greenhouse-gas-emissions-typical-passenger-vehicle (accessed Oct. 21, 2020).

[14]. J. S. M. Ali, S. M. Kashif, M. S. I. S. Dawood, and A. A. Omar, "Study on the effect of window opening on the drag characteristics of a car," Int. J. Veh. Syst. Model. Test., vol. 9, no. 3–4, pp. 311–320, Jan. 2014, doi: 10.1504/IJVSMT.2014.066502.

[15]. K. C. Nikam, L. D. Jathar, and S. L. Borse, "Study of Air Flow Through Non-Air-Conditioned Bus with Open Windows Using Open Foam," vol. 3, no. 7, pp. 105–120, 2015.

[16]. İ. Şahin and A. Acir, "Numerical and Experimental Investigations of Lift and Drag Performances of NACA 0015 Wind Turbine Airfoil," Int. J. Mater. Mech. Manuf., vol. 3, no. 1, pp. 22–25, 2015, doi: 10.7763/IJMMM.2015.V3.159.